Optics & Laser Technology 47 (2013) 283–291

Contents lists available at SciVerse ScienceDirect

Optics & Laser Technology

journal homepage: www.elsevier.com/locate/optlastec

Fire flame detection based on GICA and target tracking

Jianzhong Rong [a], Dechuang Zhou [a], Wei Yao [b], Wei Gao [c], Juan Chen [d], Jian Wang [a,*]

[a] State Key Laboratory of Fire Science, University of Science and Technology of China, Hefei 230026, PR China
[b] Institute of Public Safety Research, Tsinghua University, Beijing 100084, PR China
[c] Department of Chemical System Engineering, School of Engineering, The University of Tokyo, Tokyo,113-8656, Japan
[d] Zhejiang Institute of Safety Science and Technology, Hangzhou 310012, PR China

ARTICLE INFO

Article history:
Received 15 May 2012
Received in revised form
29 August 2012
Accepted 31 August 2012
Available online 13 October 2012

Keywords:
Video fire detection
Generic color model
Cumulative geometrical independent component analysis

ABSTRACT

To improve the video fire detection rate, a robust fire detection algorithm based on the color, motion and pattern characteristics of fire targets was proposed, which proved a satisfactory fire detection rate for different fire scenes. In this fire detection algorithm: (a) a rule-based generic color model was developed based on analysis on a large quantity of flame pixels; (b) from the traditional GICA (Geometrical Independent Component Analysis) model, a Cumulative Geometrical Independent Component Analysis (C-GICA) model was developed for motion detection without static background and (c) a BP neural network fire recognition model based on multi-features of the fire pattern was developed. Fire detection tests on benchmark fire video clips of different scenes have shown the robustness, accuracy and fast-response of the algorithm.

1. Introduction

Temperature detection and smoke detection, as the most mature fire detection technology are most widely used, but such detectors cannot satisfy fire detection requirement of some specific places such as large volume buildings, tunnel constructions, and complex buildings. With the development of the computer technology and information processing technology, detection technology based on video has gained overwhelming development in recent years. It has the advantages of fast response, wide detection range, and little environment pollution. In comparison with traditional fire detection methods, it has a broader prospect. However, these new methods are still immature, and their intelligence degree needs to be improved.

Satellite based monitoring [1,2] has been used to detect forest fires. However, the scanning period and the low resolution of satellite images make such method incapable for early fire detection. Authors in Refs. [3,4] proposed infrared (IR) based technology for fire detection. Nevertheless, these methods uses only one field sensor, making them vulnerable to false alarms. Lidar system [5,6] has also been used to detect forest fires, however, compared with fire detection method based on video image, its cost is higher and the information obtained is not intuitive, as well as higher false alarm rate [7].

Dynamic background subtraction method [4,8] is simple and the computation speed is fast, but due to its strong dependence on background image, it can only capture the edge of targets with slow moving speed and simple texture or color. Gaussian mixture model [9–12] and optical flow [13,14] method are also used for fire detection, which have the defects that: (1) relying on background frame, and the requirements of their installation are high to guarantee camera static; and (2) require huge computational resource to do a real time fire detection since their algorithm are complex. The methods of Noda and Ueda [15] based on gray-scale image processing require a stationary camera and are both designed for fire detection in some specific scenes. Cappellini et al. [16] introduced the video fire detection method based on the flame color to distinguish the fire from the smoke. Some other researchers [17–21] proposed improved color image processing techniques to achieve a real-time fire detection. The primary focus of those listed researches [17–21] are target extraction and recognition while little effort has been put to dynamic target tracking, which causes low detection rate in fire scenes with various interference sources [22].

To improve the fire detection rate, a new fire detection algorithm that combines a generic flame color model, Geometrical Independent Component Analysis (GICA) model, moving target tracking technology and multi-feature fusion model, was developed in this study, then validated using a series of benchmark fire video clips.

2. Fire detection algorithm

The proposed fire detection algorithm consists of three major steps to finally filter the fire objects:

1. Develop a rule-based generic color model to separate the flame pixels from the non-flame pixels in the RGB and SHI color space.

* Corresponding author. Tel.: +86 5513600167.
E-mail address: wangj@ustc.edu.cn (J. Wang).

0030-3992/$ - see front matter © 2012 Elsevier Ltd. All rights reserved.
http://dx.doi.org/10.1016/j.optlastec.2012.08.040

2. Develop a Cumulative Geometrical Independent Component Analysis (C-GICA) model to track the motion objects in the video sequences.
3. Develop a BP artificial neural network model to recognize the fire objects based on the multi features of the fire pattern. The multi-features are the statistical characteristics of the intensity and the Red component, the flame area and the boundary roughness.

The above three sub-models, i.e. the rule-based generic color model, C-GICA, and the fire recognition model, characterize the fire objects in terms of color, motion and pattern. Details of the sub-models developed in each step are presented as follows.

2.1. A rule-based generic color model

Flames usually have distinctive visual appearance. Except for lightly-sooting flames whose flame color can be blue, most moderately-sooting flames appear in a white or yellow color in the core flame region. Out from the high-temperature core region towards the flame edges, the flame color changes gradually from white to yellow then to red [11,23].

In this study, a total 732.3 K flame pixels are collected (the flame region identified manually) from the video images to analyze the generic color characteristics in the RGB and Saturation color space, Fig. 1 shows a few example fire images of the object under study.

Fig. 2(a) plots the red (R), blue (B) and green (G) color components for all the flame pixels, where the R and B components are separated by a 45° slope line. Fig. 2(a) indicates that the $R \geq G \geq B$ for flame pixels. Fig. 2(b) plots the R components and saturation (S) components, where the main flame region can be delimited by two thresholds: $R \geq R_T$, $S \leq fcn(R)$. Based on the observations in the color space, the following rules for the generic color model can be defined to extract the flame pixels, where only a rough application scope was given by Chen [20] previously,

$$Rule1 \quad R(x,y,t) \geq G(x,y,t) \geq B(x,y,t) \tag{1}$$

$$Rule2 \quad R(x,y,t) \geq R_T \tag{2}$$

$$Rule3 \quad S(x,y,t) \leq a^{*}R(x,y,t)+b \tag{3}$$

where the model constants are given empirically in this study, $R_T=145$, $a=-0.0023$, and $b=0.88$.

2.2. Motion detection in the video sequences

2.2.1. Geometrical Independent Component Analysis (GICA) model

Independent Component Analysis (ICA) is a method used in Blind Signal Separation (BSS) to separate the original signals from mixed signals [24–26]. ICA relies on the following assumptions [24–26]:

1. The original signals from different sources are mutually statistically independent.
2. The observed signals are deterministic (not probabilistic) mixtures of original signals.
3. The number of the observed signals is larger than that of the original signals.

A Geometrical Independent Component Analysis (GICA) was developed [26–28] based on the concept of ICA to separate the fused image through a set of geometrical transformation of in the scatter diagram. Six transformation steps were proposed by Yamaguchi et.al. [28], as diagrammatically explained in Fig. 3. Assuming that the independent signals distribute uniformly within a certain time range, the scatter diagram composed of two signals, i.e. S_1 and S_2, has the rectangular shape shown in Fig. 3 (a). Assuming that the observed signals are linear mixture of the two independent original signals ${S_1}^{(0)}(t)$ and ${S_2}^{(0)}(t)$ it has,

$$\begin{pmatrix} {S_1}^{(1)}(t) \\ {S_2}^{(1)}(t) \end{pmatrix} = \begin{pmatrix} 1 & \alpha \\ \beta & 1 \end{pmatrix} \begin{pmatrix} {S_1}^{(0)}(t) \\ {S_2}^{(0)}(t) \end{pmatrix} \tag{4}$$

The observed signals may form a scatter diagram shown in Fig. 3(b). The retrieval process is to obtain the original independent signals through a set of linear geometrical transformations from the scatter diagram in Fig. 3(b) to that in Fig. 3(a).

1. Move the scatter diagram in Fig. 3(b) parallel so that the position of $(\min({S_1}^{(1)}(t)),\min({S_2}^{(1)}(t))$ is located at the origin.
2. Rotate the scatter diagram in Fig. 3(c) by $-\theta^{\circ}$ toward the ${S_1}^{(2)}(t)$axis, resulting in the scatter diagram in Fig. 3(d).
3. Re-originate the center of segment between the position of $(\max[{S_1}^{(3)}(t)],0)$ and the origin on the ${S_2}^{(3)}$axis, as shown in Fig. 3(e).
4. Shear the parallelogram of the scatter diagram in Fig. 3(e) toward the ${S_2}^{(4)}$axis to produce a lozenge shape as in Fig. 3(f).
5. Square the lozenge shape as shown in Fig. 3(g).
6. Finally, rotate the square by 45°to obtain the scatter diagram in Fig. 3(h), where the original independent signals can be retrieved by the projection of the mixed signals on each coordinate.

An example is given in Fig. 4 to show the separation process of fused images using GICA. The RGB colored images in Fig. 4(a) were converted into gray images in Fig. 4(b). Then mix the two independent images in the ratios of 5:5 and 6:4 to produce the fused images in Fig. 4(c). The separated images of the fused images by GICA transformations are shown in Fig. 4(d), which is close to the original independent images in Fig. 4(b). Firstly, the mixed two gray images were mapped into the scatter space, then through a series of geometrical transformation steps shown in Fig. 3, the component-independent scatter map was

Fig. 1. Some example fire images used for color statistics.

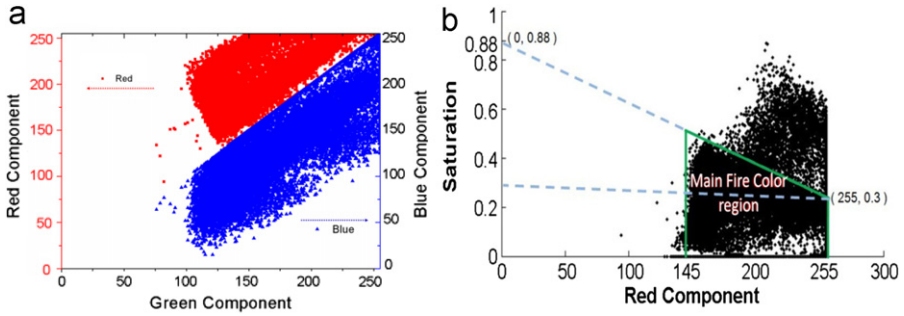

Fig. 2. Flame color presented in the color spaces of (a) R/G and B/G color, and (b) saturation and red component. (For interpretation of the references to color in this figure, the reader is referred to the web version of this article.)

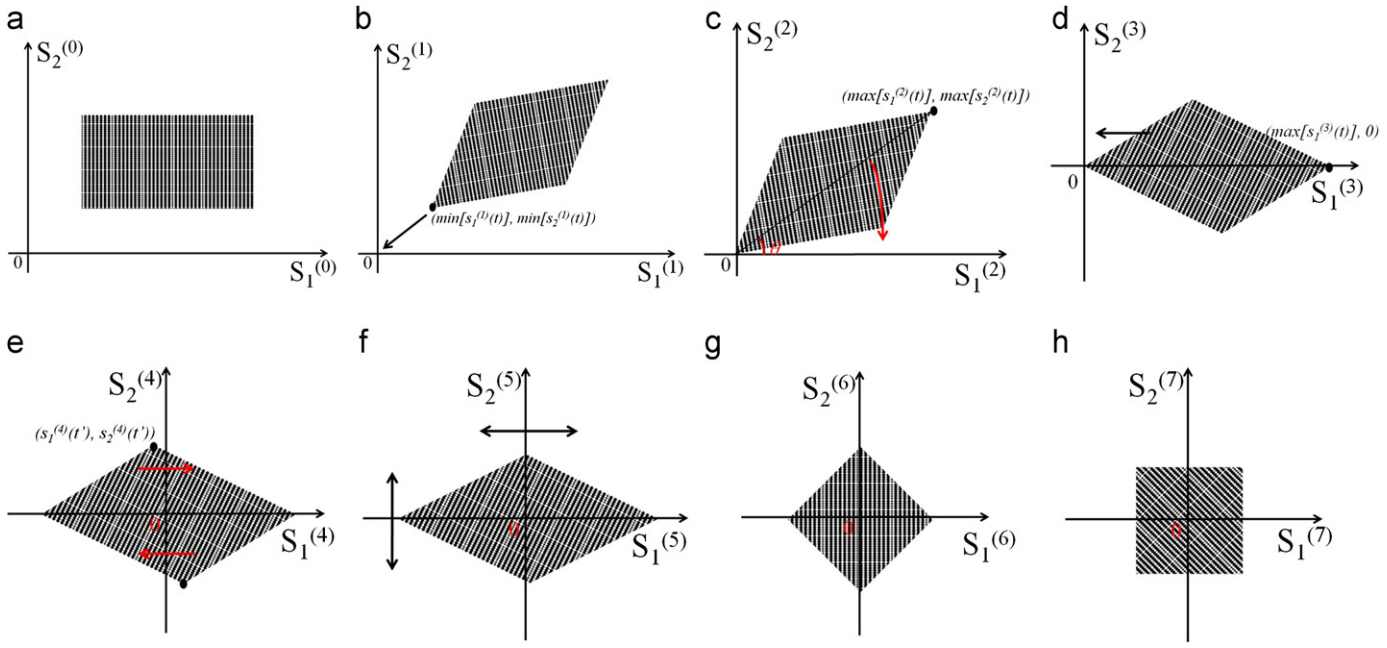

Fig. 3. Transformation steps in GICA.

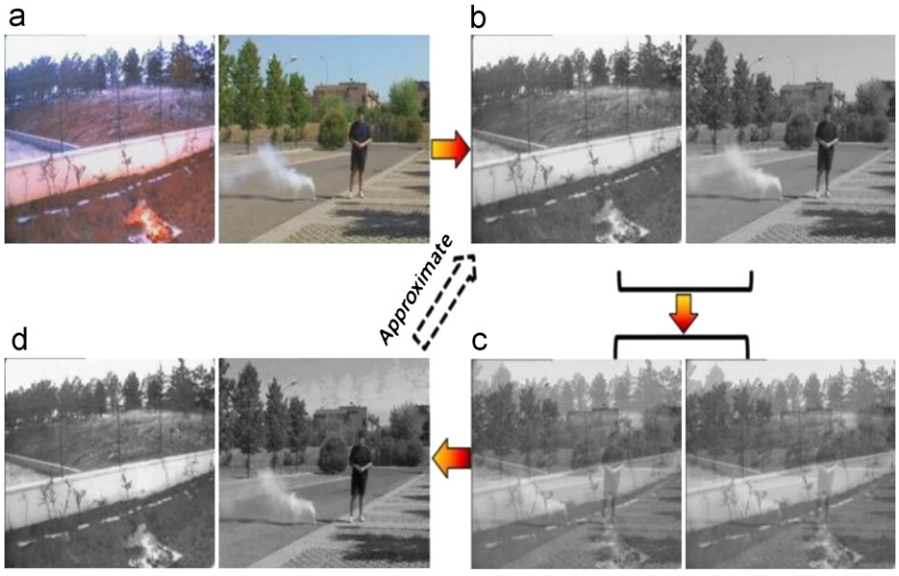

Fig. 4. Image fusion and image separation. (a) RGB color space images, (b) Gray images, (c) Fused images, proportions are 5:5, 6:4 and (d) GICA separation images.

obtained and remapped from the scatter space to the signal space to finally reproduce the separated images in Fig. 4(d).

Table 1 compares the Peak Signal to Noise Ratios (PSNR) and CPU running times between the GICA and the classical FastICA, which is based on a fixed-point iteration scheme maximizing non-Gaussianity as a measure of statistical of statistical independence [29]. The PSNR is close, but GICA significantly reduces the running time than the FastICA. As the image size increases, the running time of FastICA increases much greater than GICA. The short running time for GICA would gain more advantage in real-time video fire detection.

2.2.2. Cumulative Geometrical Independent Component Analysis (C-GICA) model

Motion detection by GICA assumes that the image is a mixture of two independent signal layers, the background layer and the moving object layer. An example was given below. Motion detection by GICA is through a series of geometrical transformations described in Section 2.2.1 to retrieve the decomposed motion objects from the stationary background to the maximum extent.

Fig. 5(a) and (b) shows two sequent images frames from a fire video, whose gray-level scatter diagram was jointly plotted in Fig. 6(a). Because the camera is fixed in a stationary view angle, the signals in the scatter diagram are concentrated around the diagonal of 45°. A small quantity of pixels scattered outside the diagonal region were mainly the pixels of moving objects. Rotate the scatter diagram of observed signals by 45°, then use thresholds $T1$ and $T2$ to exclude the signals of stationary background from those of moving objects, as shown in Fig. 6(b). The image of moving objects can be obtained through inversely mapping of the scatter points to the image, as shown in Fig. 5(c). Because of the periodic puffing of the flames, in order to accelerate the speed, it is needed to reversely transform $Y1$ or $Y2$ component to directly obtain the moving region [30].

The absolute values for the thresholds $T1$ and $T2$ were empirically determined as varying between 5 and 30 for different fire scenes to successfully decompose the moving fire objects. A medium value of 10 was selected, i.e. $T1=-10$ and $T2=10$. Fig. 9 shows the motion detection of the fire objects by GICA. For the example images of 1440×1080 pixels, a short running time, 106.02 ms, was consumed when using GICA, which greatly accelerates the detection speed.

As can be seen, the motion detection by GICA requires a static fire background, i.e. the view angle of the camera be fixed. In order to increase the robustness of the motion detection, a Cumulative GICA (C-GICA) model was developed for fire videos with non-static backgrounds. The C-GICA model was described by the following mathematical expressions.

The moving region is determined using GICA transformation with thresholds Th_0,

$$G_t(x,y)=\begin{cases} f_t(x,y) & (G(f_t,f_{t-1})\geq Th_0)\\ 0 & (G(f_t,f_{t-1})<Th_0)\end{cases} \tag{5}$$

where $Th_0=10$ is the GICA threshold, G_t represents the moving region. The numerical scope of G is between 0 and 255, where 0 represents static region and non-zero values represent the moving region.

Then apply the following equation to each pixel in the image to judge the color model,

$$C_t(x,y)=\begin{cases} 1 f_t(x,y)\in C_m\\ 0 f_t(x,y)\notin C_m\end{cases} \tag{6}$$

where C_m is the color decision model aforementioned, $C_t(x,y)$ is a binary matrix which meets the three rules of the generic color model, the digital number 1 means that the current pixel satisfy the flame color conditions, while 0 means non-flame pixel.

The C-GICA is calculated by

$$G_{ct}(x,y)=\sum_{t=1}^{N}\{G_t(x,y)\ \ C_t(x,y)\}, \tag{7}$$

where $G_{ct}(x,y)$ is the cumulative matrix of $C_t(x,y)$, and in this study 11 sequent images frames were analyzed, i.e. $N=10$.

The moving object $M_t(x,t)$ is determined by a threshold $Th_1=500$,

$$M_t(x,y)=\begin{cases} 1 & if\ \ G_{ct}(x,y)\geq Th_1\\ 0 & else\end{cases} \tag{8}$$

The fire pixels extracted using the C-GICA model were processed by a 2×2 pixel median filtering (filter) and an eight-field morphology erosion and dilation to removed burr pixels. Then an eight-field grow method was to get full flame. Fig. 7 shows the processing steps of fire detection in example video sequences by C-GICA.

Table 1
Comparison results between GICA and FastICA.

Image size	320ge s				1440e size			
Methods	GICA		FastICA		GICA		FastICA	
PSNR (dB)	+26.1	+32.8	+11.5	+34.35	+26.1	+32.3	+30.2	+26.1
Runing time (ms)	29.30		285.57		569.58		5862.48	

Fig. 5. Two sequent image frames from a fire video, and the motion area detected by GICA.

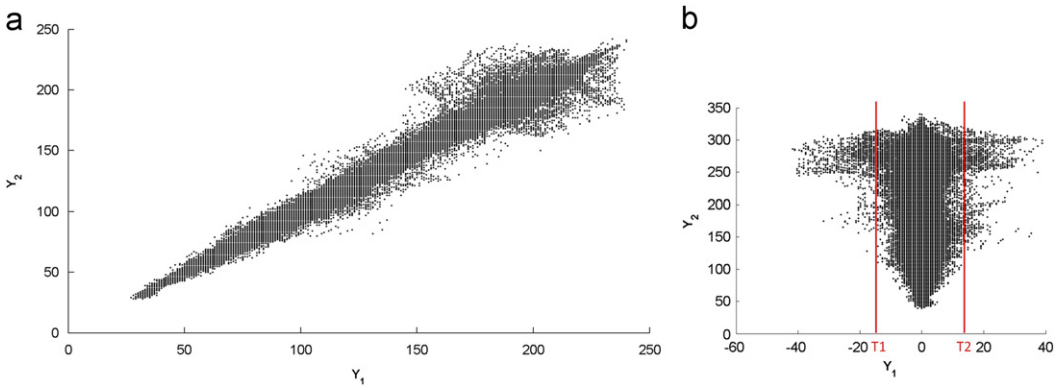

Fig. 6. GICA transformations for fire detection.

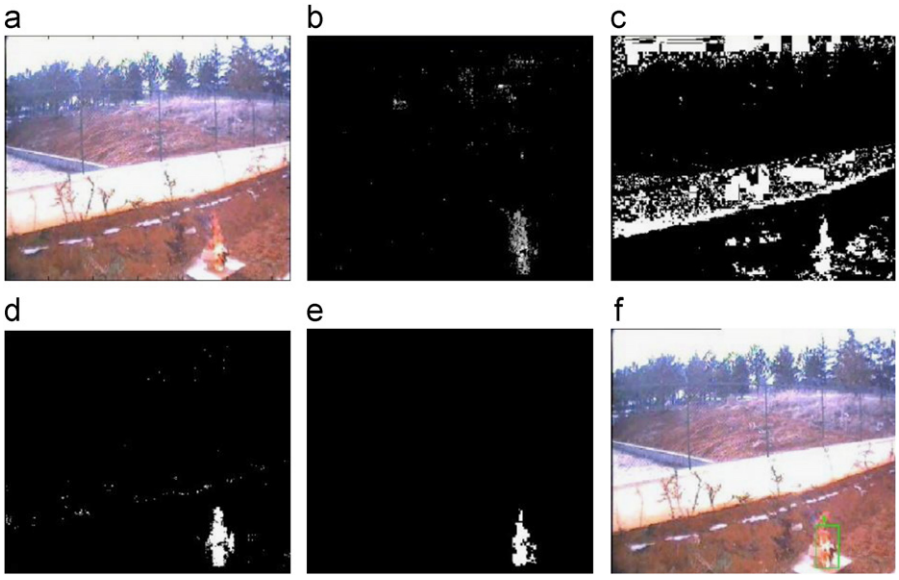

Fig. 7. Fire detection in example video sequences by C-GICA.

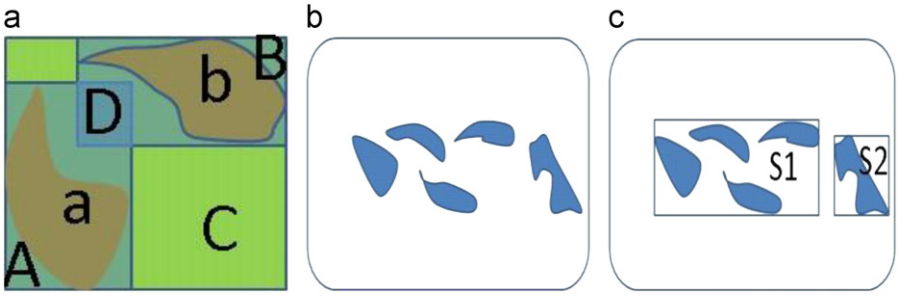

Fig. 8. (a) the merge of target a and target b into C, the merge of (b) multi-targets into (c) whole targets.

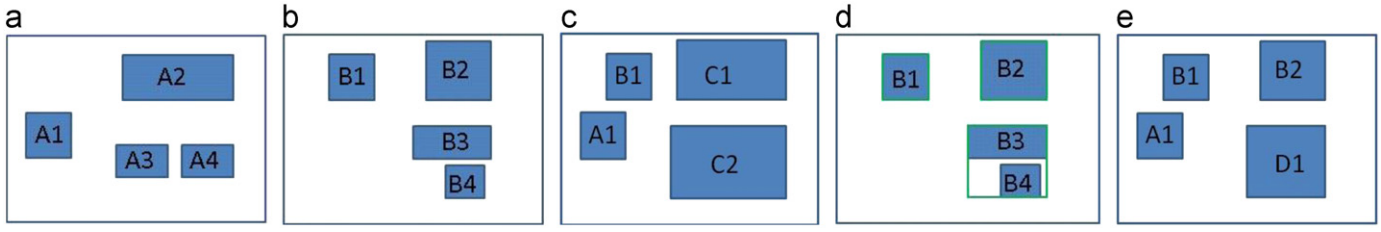

Fig. 9. A simple diagram of multi-target tracking of moving regions. (a) P1, (b) P2, (c) P3, (d) P4 and (e) P5.

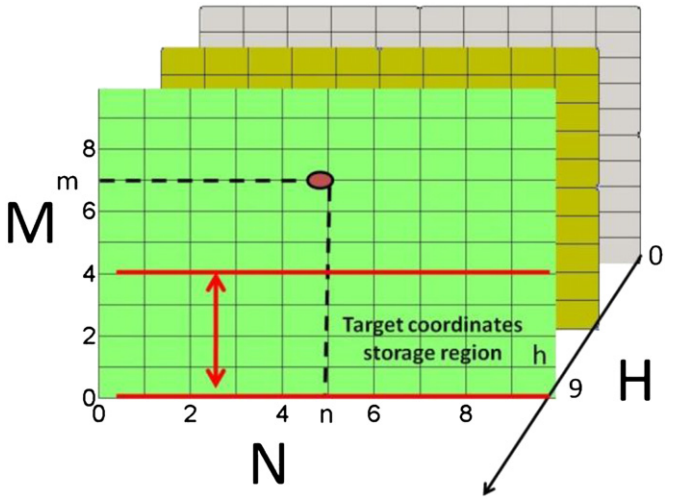

Fig. 10. Schematic diagram of the 3-D matrix structure storing object information.

2.2.3. Multi moving target tracking

Target tracking algorithm is used to build the correlation for each moving object among sequent video frames, in preparation for object reorganization in the next step.

Multi-targets are merged if their fit rectangular regions intersect with each other. An example is given in Fig. 8, where the minimum rectangular region A containing target a, and the minimum rectangular region B containing target b, have a common intersection region D, there for the target a and b can be merged into a whole region C. Repeat the merging procedure for all the individual targets in the image frame, until no target can be merged. Fig. 8(b) and (c) gives an example of multi-target merging.

Fig. 9 gives an example of multi-target tacking, if there are 3-D matrix and the current image, according to the 3-D matrix,P1 can be restored out, the current image can also be formation P2,then multi-target tracking, P1 and P2 merged into P3,which is an transition 3-D matrix; P4 can be transformed into a new 3-D matrix to replace the old 3-D matrix, and P5 is labeled as current image where A1 represents the disappearing target in current image, B2 is an emerging target, A3 and A4 are exhibited as two targets in the old 3-D matrix. Because of the existence of A3 and A4, B3 and B4 are finally merged into a single target D1.

2.2.4. Data structure for multi-targets tracking

A 3-D matrix with the size of $M \times N \times H$ was used to store the object information, i.e. the location and characteristics of the objects, as denoted in the schematic diagram (Fig. 10). In the matrix, the row dimension M is used to distinguish different characteristics, the column dimension N is to distinguish different goals, and the layer dimension H is to distinguish different frames. All of object coordinates are stored in M1–M4 rows of the first H1 layer, 1st–4th rows of 2nd Hth layers are not used.

2.3. Fire recognition model based on multi-features of the fire pattern

2.3.1. Surface coarseness

Filter banks are usually used in the texture analysis [31]; however the texture pattern of a fire image is hard to be described by any model. In this study, the statistical means, variances, skewness values, Kurtosis values of the intensity and the red component respectively are used to characterize the coarseness of the fire pixels.

$$\mu = E[x] \tag{9}$$

$$\sigma^2 = E[(x-\mu)^2] \tag{10}$$

$$sk = \frac{E[(x-\mu)^3]}{\sigma^3} \tag{11}$$

$$ku = \frac{E[(x)^4]}{E[(x)^2]^2} \tag{12}$$

2.3.2. Randomness of area size

The flame area was calculated using statistical binary image. Its computation formula

$$S_i = \sum_{x=1}^{M}\sum_{y=1}^{N} f^i_{bina}(x,y) \tag{13}$$

where $f^i_{bina}(x,y)$ is the binary image of the moving target, with 1 representing the moving target itself, 0 representing the static background, M and N represents the length and width of the moving target.

Fire has the property of flickering, which would increase or decrease the flame area. The variance of the normalized flame area S^*can be used to characterize the puffing frequency of the fire,

$$S^* = [E(S'-\mu_s)^2] \tag{14}$$

$$S' = \frac{S_i}{\max(S)}, \quad \mu_s = E(S) \tag{15}$$

2.3.3. Boundary roughness

Fourier Descriptor (FD)is usually used to characterize the fire shapes, but it is time-costing and resource-consuming thus not suitable for fast-response fire detection. Besides, the detailed shape characteristics described by FD is not necessary needed for fire detection purpose, where only the boundary roughness is required.

In this study, the boundary roughness of the potential fire region is used as the input parameters, given by the ratio between the convex hull perimeter [32] and the perimeter,

$$B_R = \frac{P_C}{P} \tag{16}$$

where, $0 < B_R \leq 1$,convex hull perimeter P_c, and P is the perimeter of flame candidate.

2.3.4. BP artificial neural network decision system

MATLAB toolbox neural network to provide a powerful neural network design, training and simulation functions [34]. In this paper, training function using Newton BP algorithm functions, hidden neurons use ‘tansig’ transfer function, two ‘logsig’ transfer functions used for the output layer, then positive/negative signal were used for training on BP neural network, and finally realize the classification of the flame image.

3. Tests and analysis

The performance of proposed fire detection algorithm was verified in benchmark video clips of different fire scenes.

3.1. Response time and tracking algorithm testing

Fig. 11 presents the 5 image frames, No. 635, No. 669, No. 743, No. 750 and No. 751, extracted from the video of a fire beside a highway at night. In the fire video, the ignition occurs in frame No. 635, and the visible flame become observable in frame No. 669.The target tracking and recognition algorithm successfully detect the fire in the frames after ignition, with the maximum detection time ≤ 3.9 s. The fire in frame No. 743 is partially sheltered, and is completely sheltered in frame No. 750, but the algorithm still successfully marks the fire region. This is credited to the delay 3-D data structure for target tracking, where a historical trace of the fire region is tracked in the frame No. 750. Without the usage of the target tracking algorithm, fire detection in frame No. 750 would be difficult. In frame No. 751, the fire was recognized directly, super than fire detection algorithms without target tracking.

3.2. Test on different scenes

The proposed fire detection algorithm has been tests on different fire detection benchmark videos with the resolution of 320×240 (http://signal.ee.bilkent.edu.tr/VisiFire). The following tests 8 video clips, among them there are 6 fire scenarios and 2 complex interference scenarios. The 8 video clips were numbered from 1 to 8, as listed in Table 2.

The fire detection algorithm was compared with the two algorithms developed by Celik [21] and Chen [33] using on the 8 video clip. Fig. 12 presents the detection results of 8 different fire scenes. The fire regions have been successfully marked by red rectangles although against the background of various interference sources, such as red lawn, walking man, moving car lights and the ground reflection. The moving objects with the flame color characteristics are marked by green rectangles, which indicate strong interference sources to fire detection but

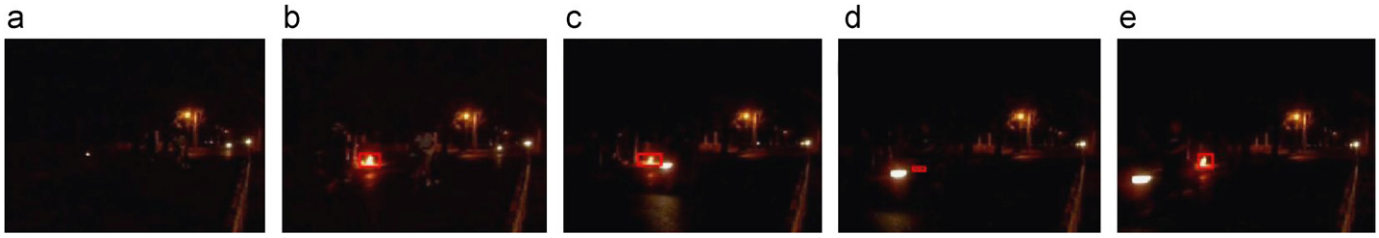

Fig. 11. Detection result of a highway fire scene, the image frames are No. 635, No. 669, No. 743, No. 750 and No. 751.

Table 2
The details of testing video clips.

Movie No.	Video frames	Flame frames	Scene descriptions
No. 1	400	400	Fire burns fiercely; cars with strong lights on the far motor road; the grass is close to the flame in color; the wall is in white, which is close to the color of flame core; people add fuels several times.
No. 2	707	630	The floor and wall are close to the flame in color; people strolled in the monitor scene; sunlight is strong.
No. 3	438	438	Fire burns fiercely in the pan against a wall; the wall color is close to that of flame; flame sways obviously under windy weather; sunlight is weak.
No. 4	244	244	Forest fire
No. 5	199	199	Forest fire
No. 6	218	218	Forest fire
No. 7	159	0	Road scene in the night; several residences with light on; a pedestrian carrying good on the roadside; passing cars on the road with strong light reflection.
No. 8	154	0	Road scene in the night; a reflecting car top close to the camera; card coming from the far with strong light reflection on the road.

Fig. 12. Test images in the 8 fire scenes. (For interpretation of the references to color in this figure, the reader is referred to the web version of this article.)

Table 3
Fire detection rates for the 8 fire scenes.

Video No.	1	2	3	4	5	6	7	8
Video frames	386	616	424	230	185	204	145	150
Fire frames	386	616	424	230	185	204	0	0
Celik detection frames	225	505	318	215	178	195	82	80
Chen detection frames	350	575	417	220	180	196	112	125
Current detection frames	350	480	387	228	180	185	52	10
Celik detection rate (%)	58.3	82.0	75.0	93.5	96.2	95.6	43.5	46.7
Chen detection rate (%)	90.7	93.3	98.4	95.7	97.3	96.1	22.8	16.7
Current detection rate (%)	90.7	77.9	91.3	99.1	97.3	90.7	64.1	93.3

generically non-fire targets judged from the multi-features by BP neural network model. The test results under different scenes and illumination conditions have shown the robustness and accuracy of the proposed detection algorithm.

Table 3 compares the fire detection results using the current proposed algorithm and the two algorithms by Celik [21] and Chen [33] for the 8 testing videos.

From Table 3, it is seen that the fire detection rates by Celik algorithm [21] and Chen algorithm [33] are generally high from some fire scenes in the video clips, e.g. the Celik detection rate for No. 6 is 95.6% and the Chen detection rate for No. 3 is 98.4%, but are low for some other scenes, e.g. the Celik detection rate for No. 7 is only 43.5% and the Chen detection rate for No. 8 is even low 16.7%. Thus it can be concluded that the Celik algorithm [21] and Chen algorithm [33] have strong dependence on the scene and low robustness, while the current proposed algorithm shows a good robustness for different scenes. The difference in fire detection rates from the 3 algorithms can be due to:

1. Celik [21] used single Gauss model based background remove method to detect the moving regions, then judged 6 color features in the YCbCr space to detect the fire target. Because the generic color model adopted by Celik [21] is based on the statistical data of forest fires, which is good at detecting forest fires but limits its application to other fire scenes. As confirmed in Table 3, the detection rate by Celik algorithm [21] for forest fires is in overall higher than for other fire scenes.
2. Chen [33] adopted double difference algorithm in combination with 3 color decision equations to detect the fire targets. The generic color model by Chen [33] is theoretically derived in the HIS color space and then calibrated by experimental data, thus has a good robustness for different fire scenes. The double difference algorithm through multi-thresholds decision is a better moving region detection method. According to the definition of Chen [33], the moving targets with color close to the flame color will be claimed as fire targets. Obviously Chen's algorithm [33] will have higher missing rates for video 1–6. Due to the simplicity of the decision process, Chen's algorithm [33] is difficult to be applied to complex fire scenes but only for fire monitoring in some specific or simple fire scenes.
3. The current proposed algorithm also has a slight higher missing rate than Chen's algorithm [33], but has a low false alarm rate in the fire detection tests. Two reasons can be attributed: on one hand a statistical concept was adopted in the fire detection, i.e. at least 10 frames from the first frame are required to extract the fire characteristics; on the other hand, the BP neural network training for the extraction of fire characteristics may be insufficient to misjudge the fire as other targets.

In summary, compared with Celik algorithm [21] and Chen algorithm [33], the current proposed algorithm has better applicability and robustness.

4. Concluding remarks

In this study, a new fire detection algorithm in terms of color, motion and pattern characteristics for fire video clips has been developed and successfully validated in different fire scenes. The main conclusions are given as follows:

1. A rule-based generic flame color model was developed based on analysis on a large quantity of fire pixels.
2. Compared with the traditional Geometrical Independent Component Analysis (GICA) model, a Cumulative Geometrical Independent Component Analysis (C-GICA) model was developed for motion detection, which can track the historical trace of fire objects based on a delay data structure and does not require static background fire flame motion detection.
3. A BP artificial neural network model with the inputs of multi features of the fire images, such as the statistical characteristics of the intensity and the red component respectively, the flame area and the boundary roughness, was developed to recognize the fire objects.
4. Successful fire detection tests on the benchmark video clips of different fire scenes have shown the robustness, accuracy and fast-response of the detection algorithm.

Acknowledgements

This research was supported by the Key Program of National Natural Science Foundation of China (no. 51036007) and Research Fund for the Doctoral Program of Higher Education of China (Grant No. 20103402110009).

References

[1] Zhanqing L, Nadon S, Cihlar J. Satellite detection of Canadian boreal forest fires: development and application of the algorithm. Journal of Remote Sensing 2000;21:3057–69.
[2] Zhanqing L, Khananian A, Fraser R, Cihlar J. Automatic detection of fire smoke using artificial neural networks and threshold approaches applied toAVHRR imagery. IEEE Transactions on Geoscience and Remote Sensing 2001;39:1859–70.
[3] Calle A, Casanova JL, Romo A. Fire detection and monitoring using MSG spinning enhanced visible and infrared imager (SEVIRI) data. Journal of Geophysical Research 2006;111:G04S06.
[4] Verstockt Steven, Vanoosthuyse Alexander, Hoecke Sofie Van, Lambert Peter, Walle Rik Van de. Multi-sensor fire detection by fusing visual and non-visual flame features. In: Proceedings of the 4th International Conference on Image and Signal Processing (ICISP 10) 2010. pp. 333–41.
[5] Cordoba A, Vilar R, Lavrov A, Utkin AB, Fernandes A. Multi-targetiveoptimisation of lidar parameters for forest-fire detection on the basis of a genetic algorithm. Optics & Laser Technology 2004;36:393–400.
[6] Andrei B. Utkin, Alexander Lavrov, Rui Vilar. Laser rangefinder architecture as a cost-effective platform for lidar fire surveillance. Optics & LaserTechnology 2009;41:862–70.
[7] Bellecci C, DeLeo L, Gaudio P, Gelfusa M, Lo Feudo T, Martellucci S, Richetta M. Reduction of false alarms in forest fire surveillance using water vapour concentration measurements. Optics and Laser Technology 2009;41:374–9.

[8] Töreyin Behcet Uğur, Cinbiş Ramazan Gökberk, Dedeoğlu Yiğithan, Çetin Ahmet Enis. Fire detection in infrared video using wavelet analysis. Optical Engineering 2007;46(6):067204-1–9.
[9] Grimson W, Stauffer C, Romano R, Lee L. Using adaptive tracking to classify and monitor activities in a site. Computer Vision and Pattern Recognition (CVPR 98).
[10] Yuan F, GuangXuan L, WeiCheng F, Heqin Z. Vision based fire detection using mixture Gaussian model. In: Proceedings of the 8th InternationalSymposium on Fire Safety Science, 18–22 September 2005, Beijing, China.
[11] Juan Chen Yaping He, Wang Jian. Multi-feature fusion based fast video flame detection. Building and Environment 2010;45:1113–22.
[12] Feiniu Yuan. An integrated fire detection and suppression system based on widely available video surveillance. Machine Vision and Applications 2010;21:941–8.
[13] Yu Chunyu, Zhang Yongming, Fang Jun, Wang Jinjun. Video smoke recognition based on optical flow. Proceedings of the 2nd IEEE International Conference on Advanced Computer Control (ICACC),2010, Shenyang.
[14] Kolesov I, Karasev P, Tannenbaum A, Haber H. Fire and smoke detection in video with optimal mass transport based optical flow and neural networks. In: Proceedings of IEEE 17th International Conference on Image Processing. 2010:pp. 761–4.
[15] Noda S, Ueda K. Fire detection in tunnels using an image processing method. In: Proceedings of Vehicle Navigation and Information Systems Conference, Yokohama, Japan, 1994:pp. 57–62.
[16] Cappellini Y, Mattii L and Mecocci A. An intelligent system for automatic fire detection in forests. In: Proceedings of the IEEE 3rd International Conference on Image Processing and its Applications. 1989, pp. 563–70.
[17] Yamagishi H, Yamaguchi J. Fire flame detection algorithm using a color camera. In: Proceedings of International Symposium on Micromechatronics and Human Science.1999. pp. 255–60.
[18] Phillips III W, Shah M, da Vitoria Lobo N. Flame recognition in video. Pattern Recognition Letters 2002;23(1–3):319–27.
[19] Horng WB, Peng JW, Chen CY. A new image-based real-time flame detection method using color analysis. In: Proceedings of IEEE Networking, Sensing and Control (ICNSP).
[20] Chen Thou-o (Chao-H), Cheng-Liang Kao, Sju-Mo Chang. An intelligent real-time fire-detection method based on video processing, Proceedings of 37th IEEE International Carnahan Conference on Security Technology, Taiwan:2003. pp. 194–211.
[21] Celik T, Demirel H. Fire detection in video sequences using a generic color model. Fire Safety Journal 2009;44(2):147–58.
[22] Jie Hou, Jiaru Qian, Weijing Zhang, Zuozhou Zhao. Fire detection algorithms for video images of large space structures. Multimedia Tools and Applications 2011;52:45–63.
[23] Liu CB, Ahuja N. Vision based fire detection. In: Proceedings of the 17th International Conference on Pattern Recognition (ICPR 04);2004. pp. 134–7.
[24] Comon P. Signal Processing 1994;36:287.
[25] Pope KJ, Bogner RE. Digital Signal Processing 1996;6:5.
[26] Mansour A, Puntonet CG, Ohnishi N. A simple ICA algorithm based on geometrical approach. In: Proceedings of the International Symposium on Signal Processing and its Applications (ISSPA), Kuala Lumpur, Malaysia, 13–16 August, 2001.
[27] Puntonet CG, Prieto A, Jutten C, Rodriguez Alvarez M, Ortega J. Separation of sources: a geometry-based procedure for reconstruction of n-valued signals. Signal Processing 1995;46(3):267–84.
[28] Taro Yamaguchi, Katsuhisa Hirokawa, Kazuyoshi Itoh. Independent component analysis by transforming a scatter diagram of mixtures of signals. Optics Communications 2000;173(1–6):107–14.
[29] Jutten C, Herault J. Signal Processing 1991;24:1.
[30] Kang Feng. The preliminary study of early agricultural and forestry fire deteetion method based on visual features. Zhejiang University, 2010.
[31] Jenifer P. Effective visual fire detection in video sequences using probabilistic approach. In: Proceedings of the International Conference on Emerging Trends in Electrical and Computer Technology (ICETECT). March 2011:pp. 870–5.
[32] Barber CB, Dobkin DP, Huhdanpaa HT. The Quickhull algorithm for convex hulls. ACM Transactions on Mathematical Software 1996;22(4):469–83.
[33] Chen TH, Wu PH, Chiou YC. An early fire-detection method based on image processing. In: Proceedings of IEEE International Conference on Image Processing (ICIP 04). Singapore:2004. pp. 1707–10.
[34] 〈http://www.mathworks.cn/products/neural-network〉.